

Original Research

Co-Highly Expressed *SLC17A9* and *KCNH1* as Potential Prognostic Biomarkers and Therapeutic Targets in Clear Cell Renal Cell Carcinoma

Zongpan Ke^{1,2,*,†}, Zhiwang Tang^{3,†}, Deyun Shen², Yixun Liu², Yawei Shu², Xiangyu Mu², Zexuan Li², Ping Xiang², Bing Zhong³, Xuechun Hu², Ruoyun Tan^{4,*}, Jun Xiao^{2,*}

Academic Editor: Amancio Carnero Moya

Submitted: 13 February 2025 Revised: 24 March 2025 Accepted: 28 March 2025 Published: 18 April 2025

Abstract

Background: The vesicular nucleotide transporter Solute Carrier Family 17 Member 9 (SLC17A9) has recently been recognized as a significant modulator of oncogenic pathways, with its elevated expression levels being closely linked to the aggressiveness of clear cell renal cell carcinoma (ccRCC). A comprehensive understanding of the role of SLC17A9 and its associated protein markers presents substantial potential for the advancement of targeted therapeutic interventions. Methods: Our study commenced with a comprehensive bioinformatics analysis to identify differentially expressed genes potentially associated with ccRCC. Leveraging The Cancer Genome Atlas (TCGA) database, we predicted the clinical relevance of these cancer-associated genes and validated their expression profiles through multiple experimental methodologies. Functional assays were conducted to assess the impact of these genes on renal cancer cell lines. Additionally, we generated cell lines overexpressing oncogenes and identified downstream targets through RNA sequencing, followed by mechanistic exploration of their interactions. Finally, bioinformatics tools were subsequently employed to assess the diagnostic and prognostic significance of these genes in patients with ccRCC. Results: The bioinformatics analysis revealed SLC17A9 as a highly expressed oncogene in ccRCC, serving as a robust prognostic marker. Experimental validation demonstrated that SLC17A9 promotes ccRCC cell growth, proliferation, and migration. Lentivirus-based experiments revealed Potassium Voltage-Gated Channel Subfamily H Member 1 (KCNH1) as a downstream target regulated by SLC17A9 (p < 0.05). Database analysis further confirmed KCNH1's oncogenic role in ccRCC, with significant implications for patient survival. Notably, SLC17A9 and KCNH1 collaboratively drive the initiation and progression of renal cancer. Elevated expression of SLC17A9 and KCNH1 correlates with poorer prognosis (p < 0.001), whereas lower expression levels are associated with favorable outcomes in ccRCC patients. These findings highlight SLC17A9 and KCNH1 as critical biomarkers and potential therapeutic targets in ccRCC. Conclusion: SLC17A9 and KCNH1 serve as critical prognostic biomarkers in ccRCC, with SLC17A9 driving tumor progression through KCNH1 regulation. Their upregulated expression predicts poor clinical outcomes, while reduced levels correlate with improved survival, highlighting their dual role as therapeutic targets.

Keywords: carcinoma, renal cell; SLC17A9 protein, human; KCNH1 potassium channel; biomarkers, tumor; disease progression

1. Introductions

Malignant renal neoplasms is a prevalent epithelial tumor affecting both genders with high incidence rates globally [1–3]. In 2022, China recorded 77,410 new cases and reported including 46,345 deaths from renal cancer [1]. The increasing annual incidence of renal cancer is partly attributed to advancements in diagnostic technologies. At diagnosis, over 17% of renal cancer patients show metastasis [4,5]. The World Health Organization's 2022 classification identifies 16 types of renal cancer, with clear cell renal cell carcinoma (ccRCC) constituting over 75% of cases, mark-

ing it as a particularly aggressive form [6]. This underscores the critical need to discover reliable tumor markers and understand ccRCC progression mechanisms to innovate targeted treatments.

Recent investigations have highlighted Solute Carrier Family 17 Member 9 (*SLC17A9*)'s dual functionality: beyond lysosomal ATP transport, this gene critically sustains tumor cell survival by preventing organelle stress [7,8]. Its prognostic significance has been reported in various tumors including prostate, hepatocellular, gastric, and colorectal cancers [9–12]. Nonetheless, the specific prognostic role and oncogenic mechanisms of *SLC17A9* in ccRCC remain

¹Urology Department, The Second Affiliate Hospital of Nanjing Medical University, 210011 Nanjing, Jiangsu, China

²Urology Department, The First Affiliate Hospital of USTC, Division of Life Sciences and Medicine, University of Science and Technology of China, 230001 Hefei, Anhui, China

³Urology Department, The Affiiated Huaian No.1 People's Hospital of Nanjing Medical University, 223300 Huai'an, Jiangsu, China

⁴Urology Department, The First Affiliated Hospital of Nanjing Medical University, 210029 Nanjing, Jiangsu, China

^{*}Correspondence: k568898123@126.com (Zongpan Ke); tanruoyun112@vip.sina.com (Ruoyun Tan); anhuiurology@126.com (Jun Xiao)

[†]These authors contributed equally.

largely unexplored. Studies have found that drugs acting on *SLC17A9* have the potential to treat acute liver injury, type 2 diabetes, depression, steatohepatitis and other diseases [13–15], which makes this site a possible therapeutic target for ccRCC.

Potassium Voltage-Gated Channel Subfamily H Member 1 (KCNH1) is predominantly expressed in central nervous system and its expression in peripheral tissues is minimal and encodes a segment of ether-a-go-go (EAG) family. However, its overexpression and upregulation in several malignant tissues has been reported, hence implicating its role in cancer progression [16,17]. Literature suggests that inhibition of KCNH1 can hinder cancer cell proliferation [18,19] and is considered to be a potential biomarker and therapeutic target cervical cancers [20,21]. Our research identifies SLC17A9 as potential prognostic, diagnostic and therapeutic biomarker for ccRCC. This conclusion is supported by our comprehensive analysis of publicly available sequencing datasets, clinical specimen evaluations, gene set enrichment analyses, and thorough in vitro cell-based studies. We discovered pivotal role of SLC17A9 in modulation of KCNH1 expression. Additionally, our investigation explores the relationship between SLC17A9 and KCNH1 expression levels and the prognosis of ccRCC patients, utilizing public data sources. The findings of our study conclusively demonstrate pivotal role of SL17A9 in influencing KCNH1, which significantly impacts the onset and advancement of ccRCC, as evidenced by our detailed cellular experiments.

2. Materials and Methods

2.1 Cell Culture and Transient Transfection

Human renal cell lines, including the normal kidney proximal tubule epithelial cell line HK-2 and ccRCC-derived lines 786-O, A498, ACHN, and TK-10, were obtained from the American Type Culture Collection (ATCC; Manassas, VA, USA) and Shanghai Biotechnology Co., Ltd. (Shanghai, China). All cells were maintained in RPMI-1640 medium (Gibco; Thermo Fisher Scientific, Inc., Shanghai, China) supplemented with 10% fetal bovine serum (FBS; Thermo Fisher Scientific, Inc., Waltham, MA, USA) and 1% penicillin/streptomycin (Sigma-Aldridge, Shanghai, China) at 37 °C in a humidified 5% CO₂ atmosphere.

For transient transfection, negative control siRNAs and SLC17A9-specific siRNAs (sequences in **Supplementary Table 1**) were synthesized by GenePharma (Shanghai, China). Lentiviral vectors for SLC17A9 overexpression (OE-SLC17A9) and corresponding empty vectors (Control) were constructed by General Biol (Chuzhou, China). At 70% confluence, cells in 6-well plates were transfected with 3 μg siRNA or lentivirus mixed with 5 μL Lipofectamine® 2000 (Thermo Fisher Scientific) following the manufacturer's protocol. Cells were harvested 72 h post-transfection for downstream assays. All cell lines (HK-2, 786-O, A498,

ACHN, TK-10) were authenticated via short tandem repeat (STR) profiling. Mycoplasma contamination was additionally tested using the Universal Mycoplasma Detection Kit (ATCC 30-1012K, ATCC, USA) and confirmed to be negative.

High-titer lentivirus production was achieved by cotransfecting 293T cells with the SLC17A9 overexpression construct and packaging plasmids (psPAX2/pMD2.G) using Polybrene (5 μ g/mL; General Biol). Viral supernatants were collected 48 h later and concentrated to a titer of 50 MOI.

2.2 In Vivo Animal Studies

Four-week-old male BALB/c nude mice were sourced from Hangzhou Ziyuan Experimental Animal Technology Co., Ltd. (Hangzhou, China), ensuring they were maintained in specific pathogen-free conditions. The Institutional Animal Care Committee of USTC First Affiliated Hospital approved all animal protocols (No. 2023-N(A)-001), and the study was carried out in compliance with ARRIVE guidelines. To evaluate the oncogenic role of *SLC17A9*, a subcutaneous xenograft model was established using 4-week-old male BALB/c nude mice (n = 10 total, 5/group). Mice were randomized into two groups:

Control group: Injected with 5 $\times\,10^6$ A498 cells transduced with an empty vector.

OE-SLC17A9 group: Injected with 5×10^6 A498 cells overexpressing SLC17A9 via lentiviral transfection.

Subcutaneous tumor dimensions were quantified triweekly via vernier caliper measurements, with volumetric analysis performed using the ellipsoid formula ($V=0.52 \times Length \times Width^2$). On day 25 post-injection, mice were humanely euthanized, and tumors were excised for weight and volume measurements.

2.3 Anesthesia and Euthanasia Procedure

Surgical anesthesia was induced and maintained via isoflurane inhalation (4–5% induction, 1.5–2.5% maintenance; RWD, Shenzhen, China) with continuous monitoring of respiratory rate and reflexes. Preoperative analgesia (buprenorphine, 0.05–0.1 mg/kg s.c.) and thermoregulation (37 °C heating pad) were implemented to minimize distress.

Terminal euthanasia was performed via isoflurane overdose (5%) in a controlled environment, confirmed by cessation of cardiac activity and pupillary dilation. All procedures strictly adhered to the 3Rs principles (Replacement, Reduction, Refinement) and institutional ethical standards.

2.4 Collection of Clinical Tissue Samples

Clinical samples consisting of ccRCC (n = 3) corresponding to adjacent non-cancerous kidney (n = 3) were received from the Urology department, Anhui provincial hospital, USTC first affiliated hospital. This collection took place between 2021 and 2023. Informed consent was duly acquired from patients or their families/legal guardians.



The collection of these samples followed ethical protocols and was approved by the ethical review board of the institution, adhering to the guidelines of the Helsinki Declaration (Ethical Number: No.2023KY175).

2.5 RNAs Extraction and Quantitative Real-Time Polymerase Chain Reaction (qRT-PCR)

Extraction of total RNA was performed as per standard protocol of Quick purification kit (ES Science Shanghai, Shanghai, China). Quantification and purity assessment were carried out using a spectrophotometer (Nanodrop-2000, Thermo Fisher Scientific, Inc., Shanghai, China). Reverse transcription of 1 μg RNA was carried out to synthesize cDNA using Hiscript II RT SuperMix for qPCR (Vazyme, Nanjing, China). We used SYBR® qPCR MasterMix enzyme supplied by Vazyme, Nanjing, China. Used primer sequences are given in **Supplementary Table** 1 siSLC17A9 or KCNHl mRNA relative expression was calculated using the normalization formula: 2^{-ACt} (ACt = Ct-SLC17A9/KCNH1 – CtB-ACTIN).

2.6 Cell Proliferation Array and Colony Forming Assay

After transfection, 786-0 and A498 renal cell cancer cell lines were seeded into 96-welplates and grown for 48 hours at 37 °C. After that cell counting kit-8 (CCK-8) reagent was injected into each well and further incubated at 37 °C. Subsequently, the optical densities (OD) at 450 nm wavelength were measured as per the instructions of the kit densities suppliers.

For the colony-forming assay, cells showing overexpression were seeded into six-well plates and incubated at 37 °C for two weeks. Subsequently, the colonies grown in these plates were fixed with 4% paraformaldehyde (Biosharp, Hefei, China) followed by 0.1% crystal violet (Biosharp, Hefei, China) staining. Results were quantified using ImageJ software (https://imagej.net/ij/).

2.7 Migratory Assay

Transfected cells were cultured for 24 hours in RPMI-1640 medium with added serum. After washing, the cells were resuspended and placed in the upper chamber of a 24-well cell culture plate with trans-well inserts, using serum-free medium, while the lower chamber contained serum-enriched medium. The setup was incubated at 37 °C for another 24 hours. Cells were then fixed using 4% paraformaldehyde and stained with 1% crystal violet. Cells were calculated by Olympus CK30 inverted phase-contrast microscope (Olympus, Tokyo, Japan).

2.8 Immunofluorescence and Immunohistochemical Staining

For immunofluorescence (IF), sections underwent three xylene (Sigma-Aldridge, Shanghai, China) immersions, followed by ethanol (Sigma-Aldridge, Shanghai, China) immersion (100%, 95%, 80%). After clearing, anti-

gen retrieval was achieved by incubating sections in an EDTA (Sigma-Aldridge, Shanghai, China) solution with a pH of 8.0. Irrelevant protein or particles were blocked by goat serum and then goat anti-rabbit IgG (KCNH1 1:100; Proteintech, Wuhan, China) was applied and incubated, followed by a Cy3-labeled secondary antibody (Proteintech, Wuhan, China). After DAPI (Proteintech, Wuhan, China) restaining, sections were sealed and imaged under a confocal microscope (Nikon, C2+, Tokyo, Japan).

For Immunohistochemical (IHC), paraffin sections underwent similar processing, incubated with a primary antibody (SLC17A9, 1:50; Abcam, Shanghai, China), followed by a anti-rabbit secondary antibody (Zsbio, PV-6000, Beijing, China), and DAB (Abcam, Shanghai, China) chromogen. Sections were stained with hematoxylin, differentiated blue and imaged under an optical microscope (Nikon Eclipse 50i, Nikon, Tokyo, Japan).

2.9 Western Blotting

Tissues or cells were lysed using RIPA (Beyotime, Shanghai, China) and PMSF (Biosharp, Hefei, China). 30 μg protein samples underwent SDS-PAGE (Biosharp, Hefei, China) separation and were transferred to a PVDF (Biosharp, Hefei, China) membrane. Protein samples (30 μg) were separated via SDS-PAGE and transferred onto a PVDF membrane. After blocking, the membranes were incubated with primary antibodies (SLC17A9, Abcam, Shanghai, China; KCNH1, Proteintech, Wuhan, China; GAPDH, Proteintech, Wuhan, China), followed by incubation with an anti-rabbit IgG (Biosharp, Hefei, China). Imaging was performed using a Chemiluminescence Imaging System (Clinx, Shanghai, China).

2.10 RNA Seq Analysis

RNA extraction from *SLC17A9*-overexpressing and control A498 cells used TRIzol Reagent (Thermo Fisher Scientific, Inc., Shanghai, China), with quality checks by Nanodrop (Thermo Fisher Scientific, Inc., Shanghai, China) and Qubit3.0. Ribonucleic Acid sequencing (RNA-seq) (Seqhealth, Wuhan, China) library preparation used the KC-DigitalTM kit (Seqhealth, Wuhan, China), with sequencing on a DNBSEQ-T7 sequencer. Data processing included Trimmomatic filtering, de-duplication, and mapping to the human reference genome using STAR. Differential gene expression analysis used edgeR (Seqhealth, Wuhan, China), with GO and KEGG enrichment via KOBAS 3.1 software (Seqhealth, Wuhan, China).

The genomic sequence data of this study has been submitted to the NCBI database (https://dataview.ncbi.nlm.nih.gov/object/PRJNA1194047) under the following association number: BioProject [PRJNA1194047], BioSample [SAMN42746168], and BioProject [PRJNA1194047]. The submission IDs for these records are SUB14908595 (Bio-Project), SUB14594786 (BioSample), and SUB14908595. ACKAX7.



2.11 Gene Expression Profiling Interactive Analysis (GEPIA) Database Analysis

The GEPIA database (http://gepia.cancer-pku.cn/detail.php?gene=&clicktag=survival) explored the correlation between SLC17A9 and KCNH1 using Spearman's test, with SLC17A9 on the X-axis and KCNH1 on Y-axis.

2.12 Bioinformatics Analysis

Data from the The Cancer Genome Atlas (TCGA) database (https://portal.gdc.cancer.gov/) (n = 602) were analyzed using R software to develop nomogram models. KEGG analysis was conducted to identify pathways involving *SLC17A9*. Kaplan-Meier (KM) curves assessed the prognostic significance of *SLC17A9* and *KCNH1*, with logrank tests used for comparing survival curves. Hazard ratios and 95% confidence intervals were calculated using Cox proportional-hazards models, adjusting for age, gender, and tumor stage.

2.13 Quantification and Statistical Analyses

Statistical evaluation was conducted using the paired Student's t-test and one-way ANOVA. Complemented by Kaplan-Meier survival curves. Cox proportional-hazards models were constructed with clinically established reference categories for categorical variables (e.g., T1 for T stage). Hazard ratios (HRs) reflect comparisons against these baseline groups. The outcomes are performed as the mean \pm standard deviation. Statistical significance of is denoted as follows: ns: non-significant; ***p < 0.001; **p < 0.01; and *p < 0.05.

3. Result

3.1 In ccRCC, SLC17A9 Upregulation Shows a Significant Association With Various Clinical Features

We analyzed the differential expression of SLC17A9 between non-cancerous and cancerous tissues within The Cancer Genome Atlas - Kidney Clear Cell Renal Cell Carcinoma (The TCGA-KIRC) datasets, the investigation extended to assessing SLC17A9 expression across various tumor grades and stages. Our findings indicated a higher expression of SLC17A9 in cancerous tissues compared to non-cancerous ones (Fig. 1A). A positive correlation observed between SLC17A9 expression and advance stage cancer, tumor grade (Fig. 1C) and stages as defined by American Joint Committee on Cancer (AJCC). SLC17A9 expression was elevated in lymph node-positive (N1) vs N0 tumors (p = 0.003; Fig. 1B) and correlated with advanced TNM stage (Fig. 1D). To determine the prognostic significance of SLC17A9, a Kaplan-Meier analysis was conducted. The TGCA-KIRC cohort was stratified into two groups according to SLC17A9 expression levels: high and low. The group exhibiting high SLC17A9 expression demonstrated showed poorer disease free survival (DFS) and overall survival (OS) (Fig. 1E,F). To corroborate

these findings, tumor and corresponding non-tumorous tissues were collected from patients undergoing laparoscopic radical nephrectomy. IHC analysis confirmed elevated *SLC17A9* expression in tumor tissues (p < 0.05) (Fig. 1G). Quantitative real-time polymerase chain reaction (qRT-PCR) and western blot analysis further confirmed the upregulation of SLC17A9 mRNA and protein levels in tumor tissues compared to adjacent non-tumorous (Fig. 1H,I). *In vitro* comparative studies of A498, 786-O, ACHN, and HK-2 cells reinforced these observations, showing heightened SLC17A9 expression in the cancer cell lines (Fig. 1J,K). These collective results underscore SLC17A9 as a pivotal biomarker in ccRCC, with its expression closely associated with poorer prognostic outcomes.

3.2 SLC17A9 Upregulation Promotes the Proliferation of ccRCC

In this research, A498 and 786-O underwent manipulation of SLC17A9 levels through either siRNA-mediated knockdown or lentiviral-mediated overexpression. quantified the changes in SLC17A9 at both mRNA and protein levels using qRT-PCR and western blot analysis (p < 0.05) (Fig. 2A,B and Fig. 3A,B). The impact of altering SLC17A9 expression on cellular viability was measured via CCK-8 assay. We observed a significant reduction in the proliferation of renal cancer cells following SLC17A9 knockdown (p < 0.05) (Fig. 2C), while SLC17A9 overexpression led to an increase in proliferation (p < 0.001) (Fig. 3C). Additionally, Trans-well assays indicated a substantial decrease in the migratory ability of renal cancer cells post-SLC17A9 knockdown (p < 0.05) (Fig. 2D), in contrast to an increase upon overexpression (p < 0.01) (Fig. 3D). The clone genic potential, assessed through single-cell clone assays, was also found to be enhanced with *SLC17A9* overexpression (p < 0.01) (Fig. 3E). Subsequent in vivo studies involving BALB/c nude mice showed that tumors derived from SLC17A9-overexpressing cells exhibited greater volume and weight compared to those from control groups (p < 0.05) (Fig. 3F). Collectively, these results underscore the importance of SLC17A9 as a crucial biomarker in renal cancer, influencing both the proliferation and migration of renal cancer.

3.3 SLC17A9 Upregulates KCNH1 Expression in ccRCC

In this part of the study, RNA-seq was conducted on three paired samples of A498 cells, transfected either with *SLC17A9* overexpression constructs or corresponding negative control constructs. The RNA-seq samples were subjected to quality assurance, demonstrating satisfactory outcomes (Fig. 4A). The sequenced data was analyzed to identify differentially expressed genes, which were illustrated through heatmaps and volcano plots (Fig. 4B,C). These genes underwent Gene Ontology (GO) functional enrichment analysis to discern downstream pathways under *SLC17A9* influence (Fig. 4D). The enrichment analy-



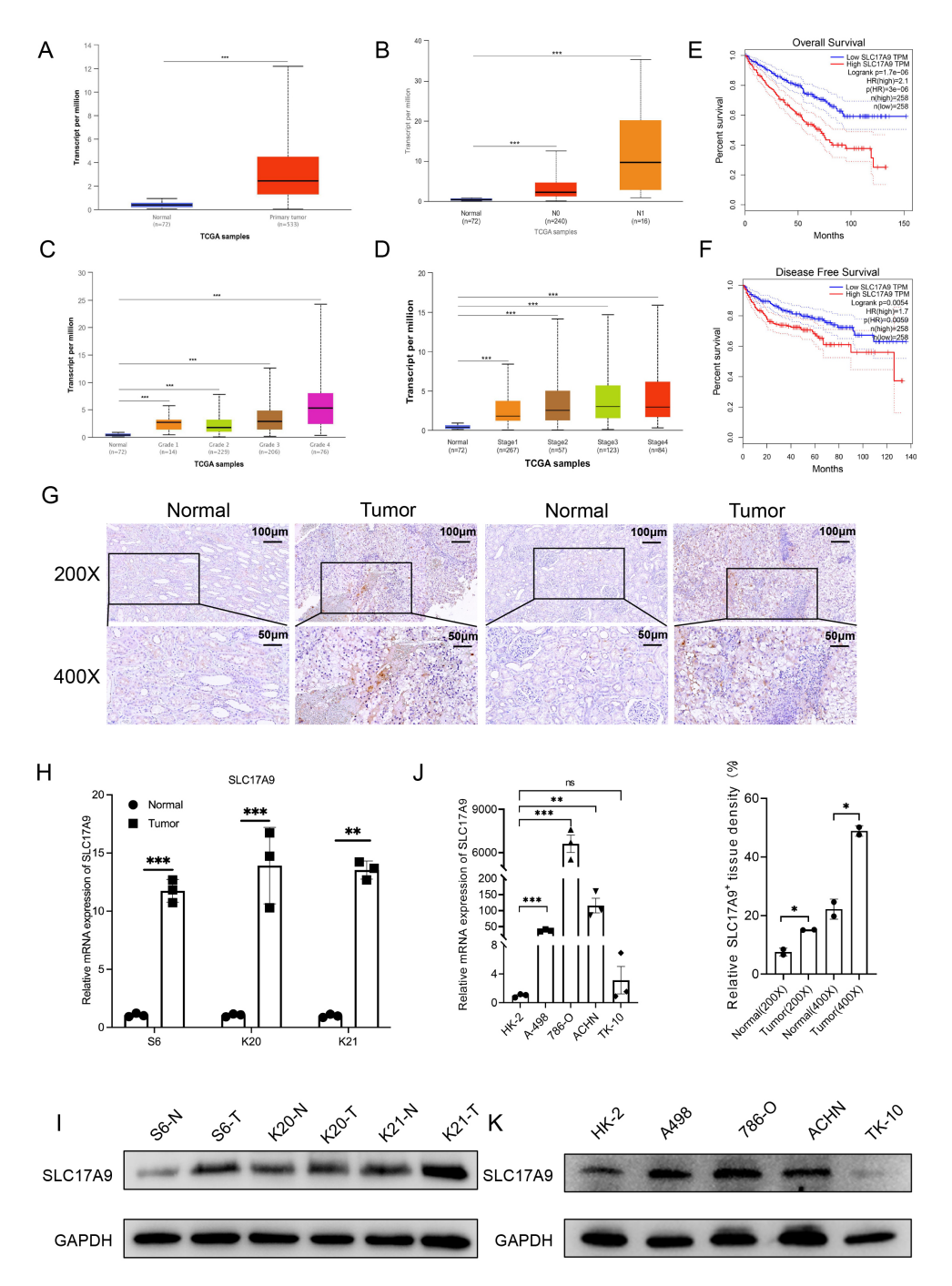


Fig. 1. Higher expression of SLC17A9 in clinical patients' samples such as tumor tissues and cells. (A) SLC17A9 mRNA expression levels in the ccRCC tissues were higher than those in the normal tissues in the TCGA cohort. (B) SLC17A9 expression levels in normal, N0 and N1 stages. (C) SLC17A9 expression levels in G grade. (D) SLC17A9 expression levels in different TNM stages in TCGA. (E) The high SLC17A9 expression group had poorer overall survival (OS) than the low expression group in the TCGA cohort, p < 0.0001. (F) High SLC17A9 expression indicated poorer disease-free survival (DFS) in the TCGA cohort, p = 0.0059. (G) Immunohistochemistry (IHC) results $(200\times, 400\times)$ of SLC17A9 in ccRCC tissues and para-cancer tissues of two patients (p < 0.05). The length of the scale bars is 100 and 50 µm. (H,I) Relative mRNA and protein levels of SLC17A9 in ccRCC tissues and adjacent normal kidney tissues. (J,K) Relative mRNA and protein levels of SLC17A9 in ccRCC cell lines. ***p < 0.001; **p < 0.01; and *p < 0.05; ns, non-significant differences. Data is represented as mean \pm standard deviation (SD). (SLC17A9, Solute Carrier Family 17 Member 9; ccRCC, clear cell Renal Cell Carcinoma; KIRC, kidney renal clear cell carcinoma; TCGA, The Cancer Genome Atlas; TNM: T, tumor; N, lymph node; M, metastasis.)

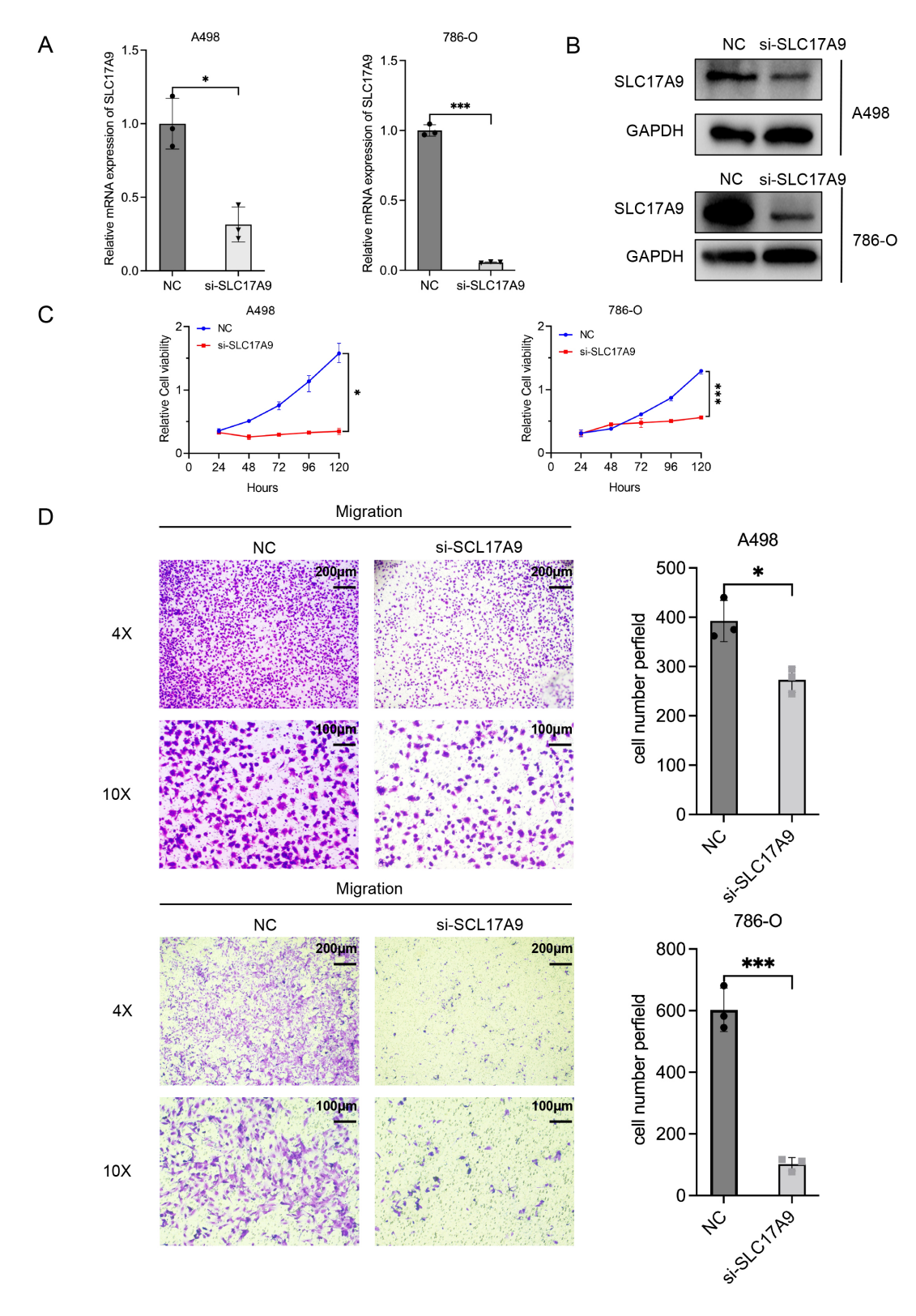


Fig. 2. SLC17A9 knocking down reduces the viability of renal cancer cell lines. (A,B) Relative mRNA expression levels and relative protein expression levels after knocking down SLC17A9 expression in A498 and 786-O. (C) The effect of SLC17A9 knockdown on A498 and 786-O cell proliferation was detected using Cell Counting Kit-8 (CCK-8) (error bars represent SEM; n = 3 independent experiments). (D) Effects of SLC17A9 knockdown on A498 and 786-O cell's migration. The length of the scale bars is 200 and 100 μ m. ***p < 0.001 and *p < 0.05. Data were presented as the mean G standard deviation (SD) from three independent experiments.

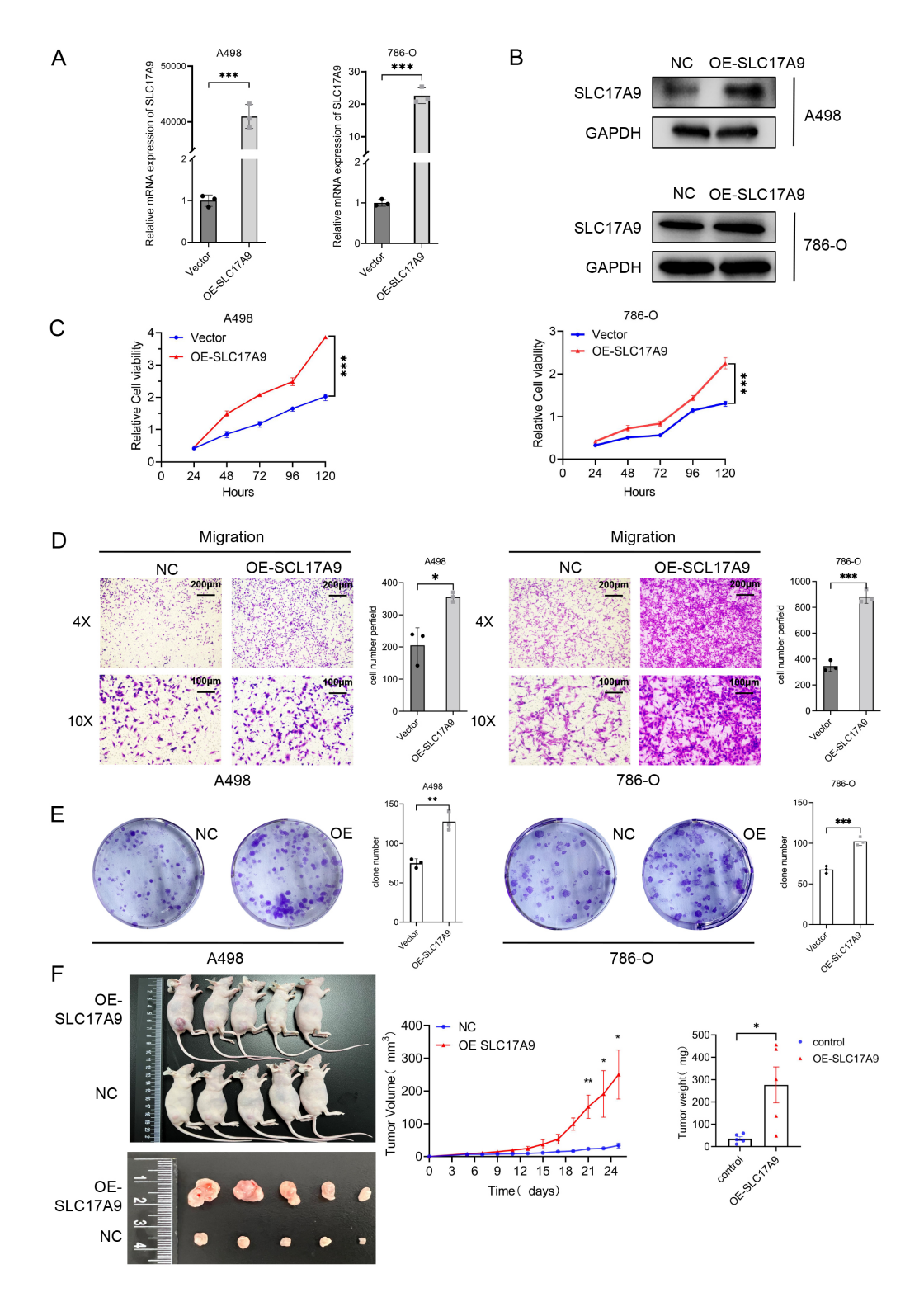


Fig. 3. Lentiviral mediated overexpression of SLC17A9 increases cellular growth, migration in vitro and fasten tumor progression in vivo. (A,B) Relative mRNA expression levels and relative protein expression levels of SLC17A9 in A498 and 786-O after overexpression of SLC17A9. (C) The effect of overexpression SLC17A9 in A498 and 786-O cell proliferation was detected using Cell Counting Kit-8 (CCK-8) (error bars represent SEM; n = 3 independent experiments). (D) Effects of SLC17A9 knockdown on A498 and 786-O cell's migration. The length of the scale bars is 200 and 100 μ m. (E) Changes in clonal capacity of cells in A498 and 786-O after overexpression of SLC17A9. (F) Subcutaneous tumor in BALB/c mice, its growth curve, and final volume and weight (n = 5). ***p < 0.001; **p < 0.01; and *p < 0.05. Data were presented as the mean G standard deviation (SD) from three independent experiments.

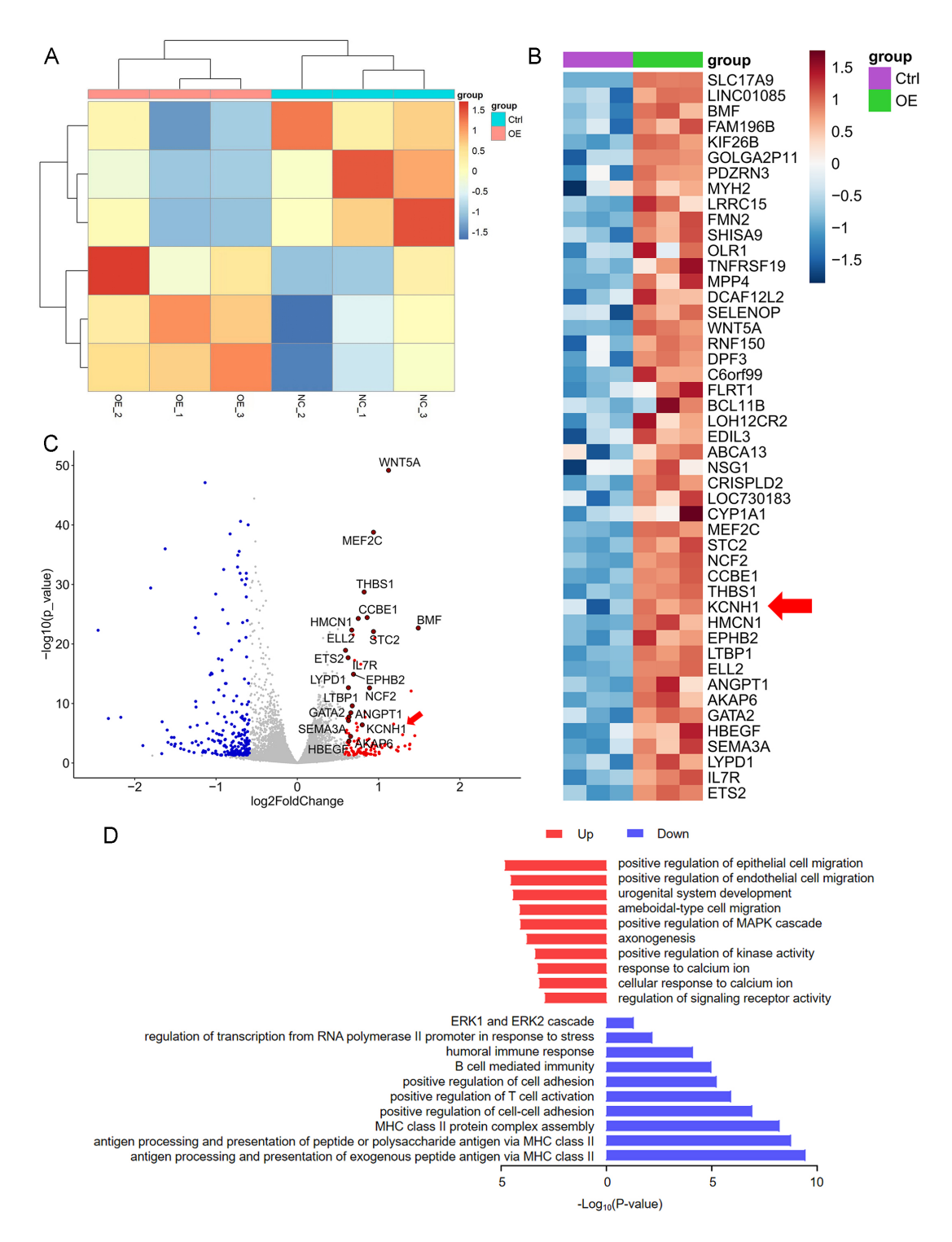


Fig. 4. Lentiviral mediated overexpression of *SLC17A9* in A498 cells shows overexpression of *KCNH1*. (A) Quality test results of cells used for sequencing. (B) Differential gene heat map. (C) Differential gene volcano map. (D) Related pathways enriched in the Gene ontology (GO) database for differential genes in A498 cells overexpressing *SLC17A9* (n = 3/group). (*KCNH1*, Potassium Voltage-Gated Channel Subfamily H Member 1).

sis led to a focus on KCNH1. Immunofluorescence studies showed elevated KCNH1 expression in tumor tissues compared to non-tumorous counterparts (p < 0.001) (Fig. 5A). An examination of the GEPIA database highlighted a correlation between SLC17A9 and KCNH1 expressions in re-

nal tumors (p = 0.045) (Fig. 5B). The prognostic significance of KCNH1 was assessed using KM curves, classifying TCGA-KIRC cohort patients into relatively low and high KCNH1 expression groups based on median levels. Results showed that KCNH1 overexpression was linked to



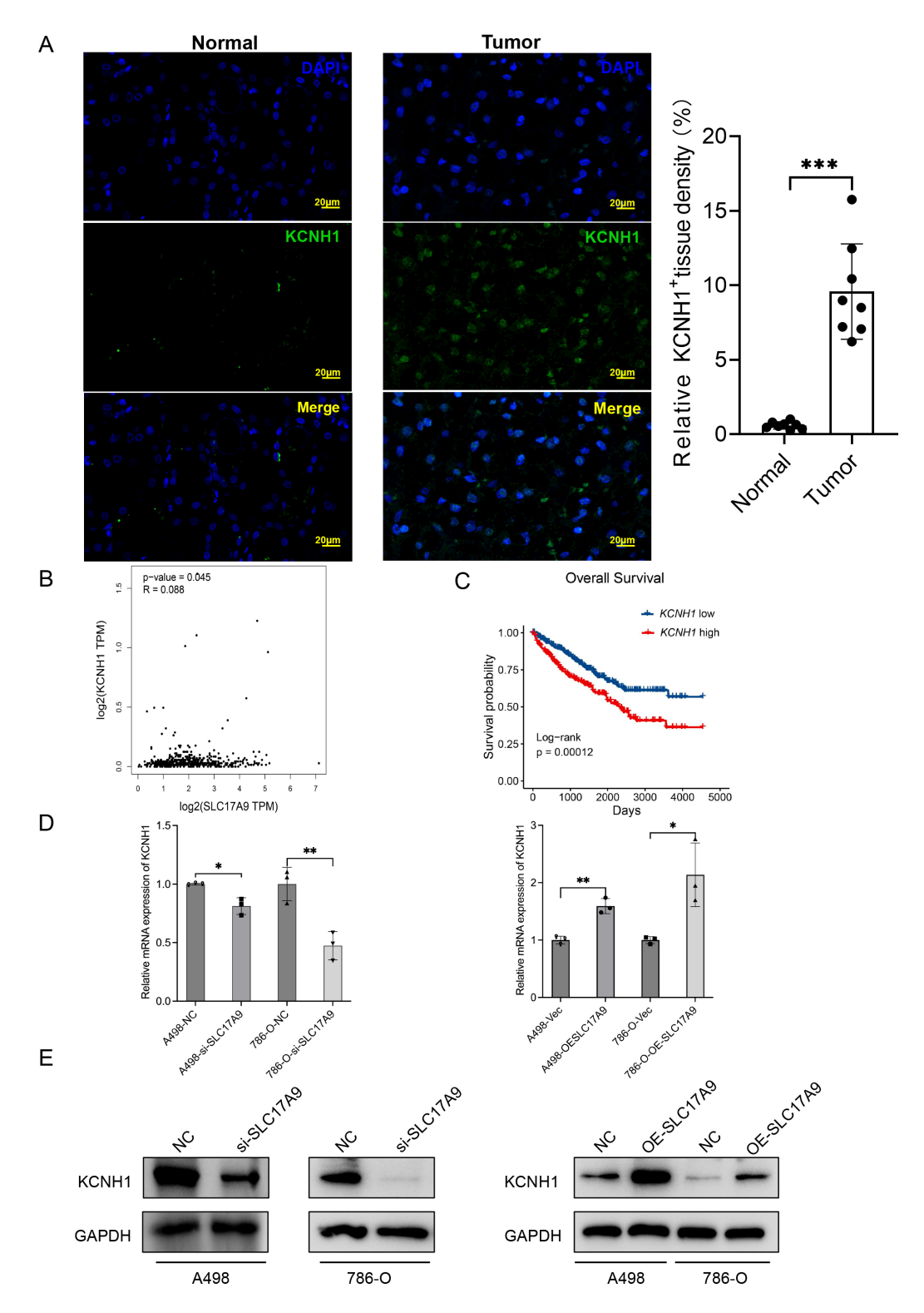


Fig. 5. KCNH1 and SLC17A9 expression are directly correlated with each other in tumor tissues, Gene Expression Profiling Interactive Analysis (GEPIA) and cell lines. (A) Immunofluorescence (IF) results ($400\times$) of KCNH1 in ccRCC tissues and paracancer tissues of the patient. The length of the scale bar is 20 µm. (B) Association of SLC17A9 and KCNH1 with renal cancer in GEPIA. (C) The High KCNH1 expression group had poorer overall survival (OS) than the low expression group in the TCGA cohort, p = 0.00012. (D,E) The mRNA expression level and protein expression level of KCNH1 in renal cancer cells overexpressing and knocking down SLC17A9 respectively. ***p < 0.001; **p < 0.01; and *p < 0.05. Data were presented as the mean G standard deviation (SD) from three independent experiments.

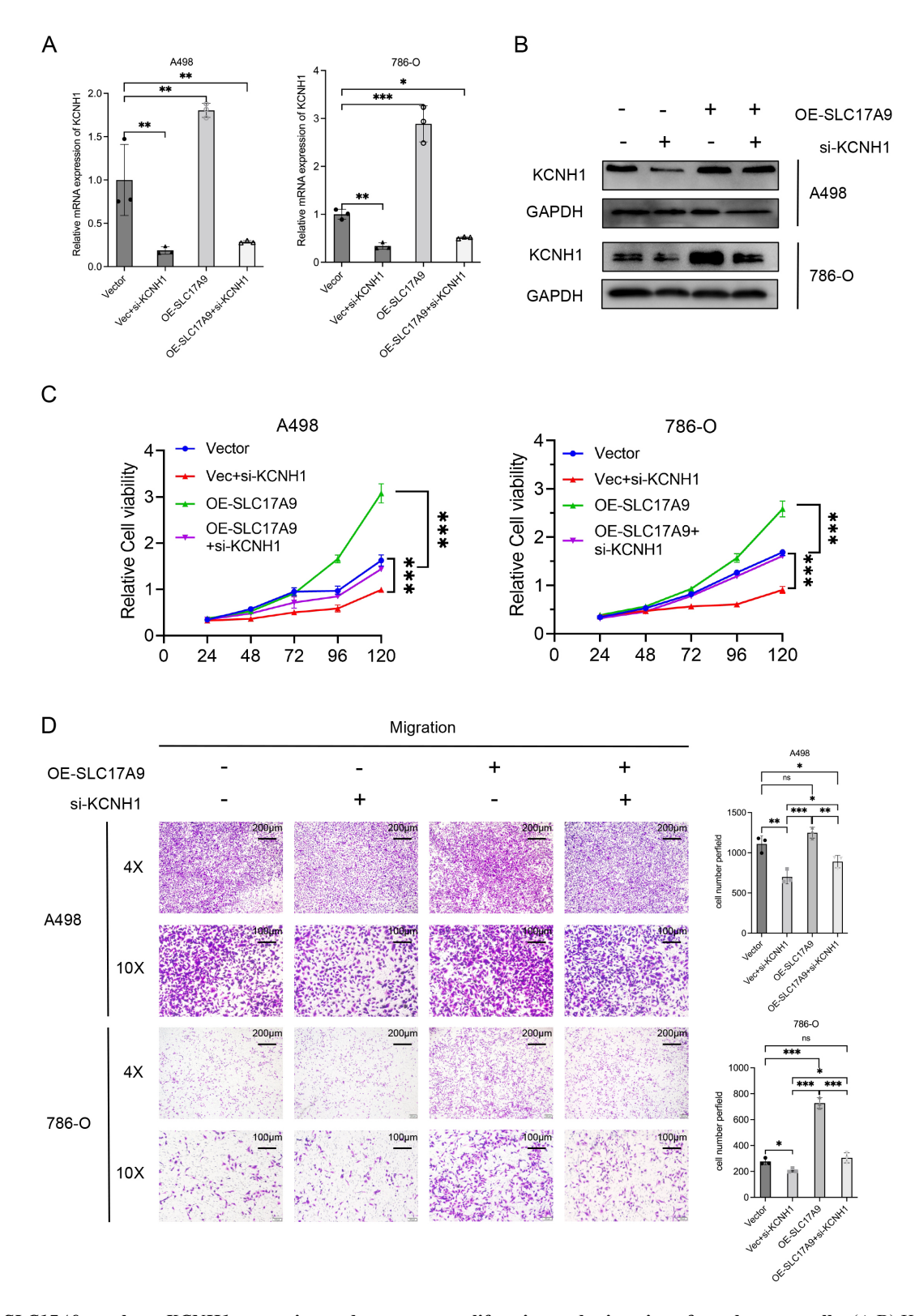


Fig. 6. SLC17A9 regulates KCNH1 expression and promotes proliferation and migration of renal cancer cells. (A,B) Knockdown of KCNH1 in renal cancer overexpressing SLC17A9, relative mRNA expression level and relative protein expression level of KCNH1. (C) Cell counting kit-8 (CCK-8) was used to detect the effect of overexpressing SLC17A9 and then knocking down KCNH1 on the proliferation of A498 and 786-O cells. (D) Effects of overexpressing SLC17A9 and then knocking down KCNH1 on the migration of A498 and 786-O cells. Scale bars are 200 and 100 μ m in length. ***p < 0.001; **p < 0.01; and *p < 0.05; ns, non-significant differences. Data were presented as the mean G standard deviation (SD) from three independent experiments.

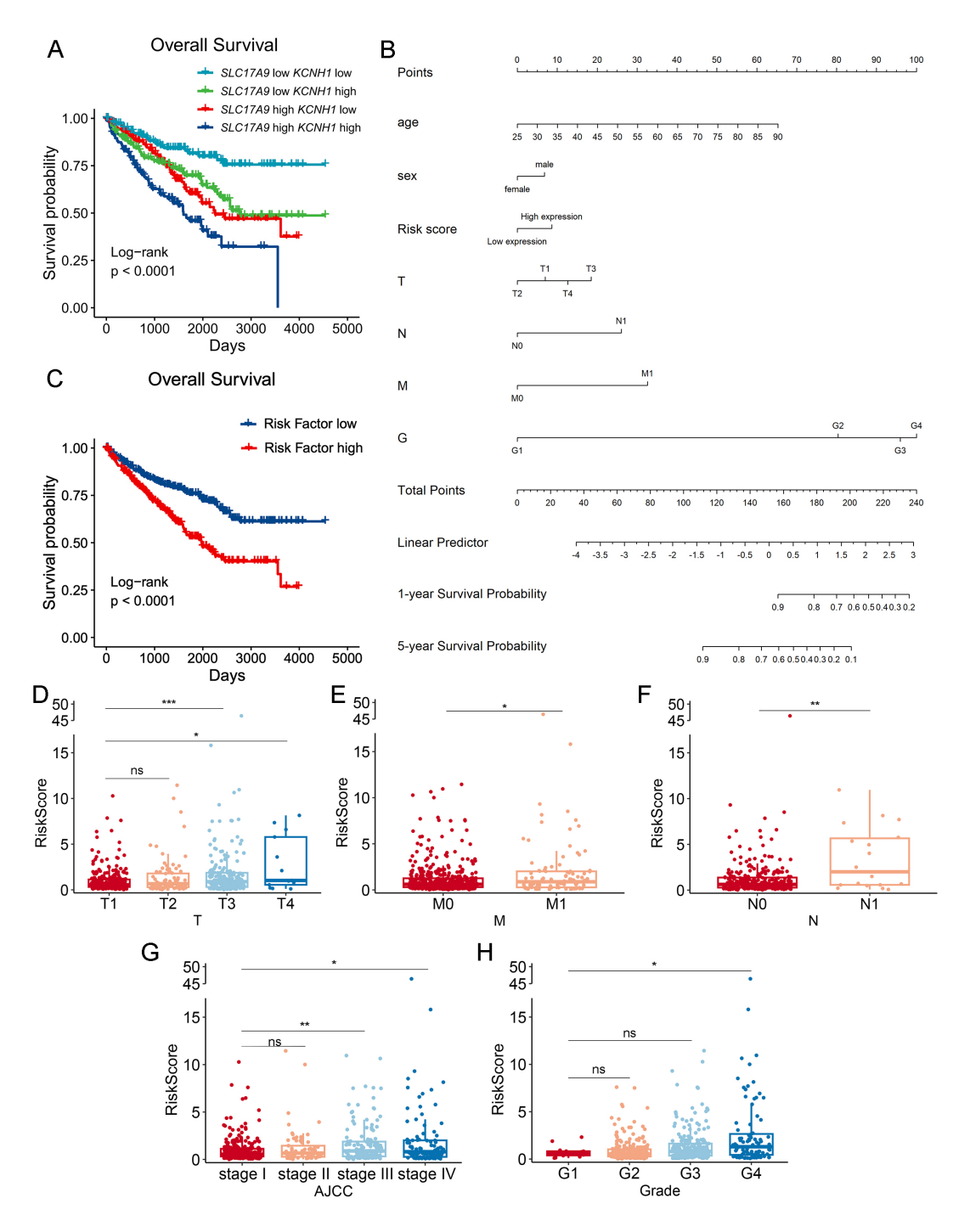


Fig. 7. Analysis of SLC17A9 and KCNH1 expression in ccRCC patients reveals prognostic significance. (A) In the TCGA cohort, the high SLC17A9 and high KCNH1 expression groups had worse OS than the low expression group of either gene. p < 0.0001. (B) The nomogram showed the combined SLC17A9 and KCNH1 risk score, TNM stage, grade, sex, and age, and predicted the 1-year and 5-year over survival (OS) possibilities of individual ccRCC patients. (C) In the TCGA cohort, the high-risk score had worse OS than the low-risk score. p < 0.0001. (D–H) The combined expression of two genes in different T stages, M stages, N stages, AJCC stages and Grade stages of ccRCC in TCGA. ***p < 0.001; **p < 0.01; and *p < 0.05; ns, non-significant differences.

poorer OS (p = 0.00012) (Fig. 5C). Further analyses using qRT-PCR and Western blotting showed that KCNH1 mRNA and protein levels were respectively downregulated in renal cancers cells with SLC17A9 knockdown and upregulated in those with SLC17A9 overexpression (Fig. 5D,E).

These results suggest a direct correlation between increased *KCNH1* expression and adverse prognosis in ccRCC, and that *SLC17A9* exacerbates ccRCC progression by promoting *KCNH1* expression.



Table 1. Univariate and multivariate analyses of unite SLC17A9 and KCNH1 expression and patient overall survival using TCGA-KIRC data (n = 602).

	Univarient analysis			Multivarient analysis		
Variables	HR	95% CI	p value	HR	95% CI	p value
Age (years) ≤60 vs >60	1.938	1.438–2.611	< 0.001	1.613	1.187–2.193	0.002
Gender Male vs Female	1.083	0.809-1.450	0.594	1.020	0.756–1.376	0.898
T stage T2/T3/T4 vs T1	3.082	2.316-4.101	< 0.001			
N stage N0 vs N1	4.186	2.329-7.522	< 0.001			
M stage M0 vs M1	4.511	3.381-6.019	< 0.001			
Grade G2/G3/G4 vs G1	2.695	1.950-3.725	< 0.001	1.638	1.160-2.313	0.005
AJCC stage II/III/IV vs I	3.949	2.918-5.346	< 0.001	2.941	2.133-4.056	< 0.001
SLC17A9 High vs Low	1.971	1.476-2.632	< 0.001			
KCNH1 High vs Low	1.739	1.306-2.317	< 0.001			
Risk Score High vs Low	2.014	1.507-2.691	< 0.001	1.611	1.197–2.167	0.002

Reference: T1; HR, hazard ratio; CI, confidence interval.

Reference categories: T1 (T stage), G1 (Grade), Stage I (AJCC), Female (gender), N0 (N stage), and M0 (M stage). Hazard ratios (HRs) represent risk relative to the reference group. TCGA-KIRC, Cancer Genome Atlas - Kidney Clear Cell Renal Cell Carcinoma; AJCC, American Joint Committee on Cancer.

3.4 SLC17A9 Promotes ccRCC Progression by Modulating KCNH1

Subsequently, in the study, KCNH1 was targeted for a knockdown in SLC17A9-overexpressing A498 and 786-O cells using specific siRNAs. The qRT-PCR analysis confirmed that siRNA-mediated KCNH1 suppression effectively reduced its mRNA levels in cells overexpressing SLC17A9 (Fig. 6A). Western blot analysis corroborated these findings, indicating a decrease in KCNH1 protein levels (Fig. 6B). Cell proliferation was assessed through CCK-8 assays, revealing that cells transfected with SLC17A9 overexpression constructs and si-negative control exhibited higher proliferation rates compared to those in negative control, SLC17A9 overexpression/si-KCNH1, and overexpression control/si-KCNH1 groups. Notably, a decline in cell proliferation was observed in the SLC17A9 overexpression/si-KCNH1 group (Fig. 6C). Furthermore, Trans-well assay indicated that cell migration was most pronounced in the SLC17A9 overexpression/si-negative control group, and this rate was reduced in the SLC17A9 overexpression/si-KCNH1 group (Fig. 6D). These results collectively indicate that SLC17A9 influences renal carcinoma cell proliferation and migration by regulating KCNH1 expression, thereby impacting ccRCC progression.

3.5 Clinical Relevance of SLC17A9-Regulated KCNH1 in the TCGA-KIRC

In our study of the TCGA-KIRC database, we categorized the patients into four distinct groups based on their levels of SLC17A9 and KCNH1 expression: high SLC17A9/high KCNH1, high SLC17A9/low KCNH1, low SLC17A9/high KCNH1, and low SLC17A9/low KCNH1. Kaplan-Meier survival analysis revealed that OS was notably reduced in patients with both high SLC17A9 and high KCNH1 expression, compared to those in the high SLC17A9/low KCNH1 and low SLC17A9/high KCNH1 groups. In contrast, patients in the low SLC17A9/low KCNH1 category had significantly better OS (Fig. 7A). For 602 patients from the TCGA-KIRC cohort, Univariate and multivariate Cox regression analyses were conducted (Table 1). The risk score was calculated using HRs from univariate Cox regression, targeting the predictive power of SLC17A9 and KCNH1 expression levels for OS in KIRC patients (risk score = HR1 \times Expression of SLC17A9 + HR2 × Expression of KCNH1). This calculated risk score, based on SLC17A9 and KCNH1 expression, was found to have significant prognostic relevance in ccRCC (Table 1). Following an approach similar to that used by Zedan Zhang et al. [22], we developed a comprehensive nomogram incor-



porating age, gender, risk score, TNM staging, and grade classification to predict 1-year and 5-year OS in ccRCC patients (Fig. 7B). The prognostic value of this risk score for the patient survival within TCGA-KIRC cohort was further validated using Kaplan-Meier curve analysis, where higher risk scores were associated with significantly shorter OS (Fig. 7C). Positive correlations were observed between the risk score and advanced stages of T, M, N, and AJCC, as well as with higher grade classifications (Fig. 7D–H). These findings highlight the critical roles of *SLC17A9* and *KCNH1* in ccRCC pathogenesis and their impact on the disease's progression.

4. Discussion

SLC17A9, a vesicular adenoside triphosphate (ATP) transport protein, regulates ATP transfer in cardiac inflammation and hypertrophy through heart-brain interaction during pressure overload. Previous studies have reported the role of *SLC17A9* in various neuropathic pain mechanisms [23,24]. *SLC17A9* is correlated with the pathogenesis of several tumors, such as colorectal adenocarcinoma [25], T-cell acute lymphoblastic leukemia [26], prostate cancer [11], lung cancer [27,28], and hepatocellular carcinoma [29].

This study examined the role of SLC17A9 in ccRCC using TCGA-KIRC datasets. The bioinformatics analysis results were validated using IHC, qRT-PCR, and western blotting analyses of clinical tumor tissues. Next, the oncogenic mechanism of SLC17A9 in ccRCC was examined. Experiments involving siRNA-mediated knockdown and lentivirus-mediated overexpression of SLC17A9 revealed its role in regulating the proliferation and migration of renal cancer cells. Previously, Weiguan Li et al. [30], demonstrated that SLC17A9 promotes ccRCC progression through a PTHLH-induced endothelial-to-mesothelial transition process. In this study, RNA-seq results suggested that SLC17A9 drives renal cancer progression via additional pathways. As shown in Fig. 4D, the upregulated pathways indicated that SLC17A9 enhances ccRCC cell migration by modulating epithelial and endothelial cell migration. Furthermore, SLC17A9 promotes renal cancer development through the MAPK cascade reaction [31] and plays a role in determining sorafenib efficacy [32]. SLC17A9 overexpression downregulated several immune-related pathways, suggesting that SLC17A9 affects ccRCC progression by modulating immune processes. The findings of this study are consistent with those of Weiquan Li et al. [30].

Among the upregulated genes, this study selected *KCNH1*, a gene associated with the pathogenesis of various cancers, such as soft tissue sarcoma [33], cervical cancer [20], colorectal cancer [34], glioblastoma [35], hepatocellular carcinoma [36], and head and neck cancers [37] has been confirmed, However, prior to this study, its specific role in ccRCC had not been investigated. Using KM survival analysis from TCGA-KIRC database, we

found KCNH1 expression to be highly correlated with survival prognosis in KIRC, with higher expression linked to poorer outcomes. Additionally, KCNH1 was found to be more highly expressed in tumor tissues than in normal tissues. Subsequent experiments on SLC17A9 overexpressed renal cancer cells revealed elevated KCNH1 levels, providing the first evidence that KCNH1 is regulated by SLC17A9 and modulates the proliferation and migration of renal cancer cells. Finally, using data from 602 cases in the TCGA-KIRC database, univariate and multivariate Cox proportional-hazards ratio analysis and risk scoring were performed, analyzing SLC17A9 and KCNH1 together for the first time. The analysis indicated that SLC17A9 and KCNH1 are important biomarkers in the development and progression of renal clear cell carcinoma. Notably, Pharmacological screening identified imipramine (IC₅₀ = $5.8 \mu M$) [38] as potent KCNH1 inhibitors, suggesting repurposing potential for ccRCC therapy, proven to reduce tumor proliferation and may enhance the combined medication effect with SLC17A9 in Vorinostat-resistant clear cell renal carcinoma [30]. Our findings provide novel insights into the SLC17A9/KCNH1 signaling pathway as a driver of ccRCC progression.

There are some limitations in this study that we need to address in the future. This study demonstrated that *SLC17A9*-regulated *KCNH1* promotes the development and progression of ccRCC but did not elucidate the underlying downstream mechanisms. Future studies must elucidate the mechanisms underlying *SLC17A9*-mediated *KCNH1* regulation and *KCNH1*-mediated ccRCC progression, as well as identify drugs targeting *SLC17A9* and *KCNH1*.

5. Conclusions

SLC17A9 and KCNH1 are significant prognostic markers for ccRCC. Additionally, SLC17A9 promotes the onset and progression of renal cancer by regulating KCNH1 expression. SLC17A9 expression was positively correlated with KCNH1 expression. The upregulation of SLC17A9 and KCNH1 is positively correlated with poor prognosis in patients with renal cancer. Conversely, SLC17A9 and KCNH1 downregulation is correlated with improved prognosis.

Availability of Data and Materials

Sequencing data associated with this manuscript is available online in NCBI database with the provided IDs. If additional information's are required, corresponding authors will provide on reasonable request as per journal and institution policy.

Author Contributions

ZK, ZT and DS: experimental design and execution. YL, DS and ZL: performed bioinformatics analyses. XM, YS and YL: sample collection and data analysis. XH, BZ



and PX: manuscript drafting with the help of all author, provided financial support for the research and interpretation of data and contributed to editorial changes in the manuscript. RT: designing the research study, performed the research, analyzed the data, participated in experiments, reviewed and edited the final draft of the manuscript. JX: data analysis, validation, and review of manuscript. All authors contributed to editorial changes in the manuscript. All authors read and approved the final manuscript. All authors have participated sufficiently in the work and agreed to be accountable for all aspects of the work.

Ethics Approval and Consent to Participate

This study was approved by the Ethics Committee of the USTC First Affiliated Hospital (Ethical Number: No.2023KY175) in accordance with the Declaration of Helsinki. Written informed consent was obtained from patients or their families/legal guardians. The Institutional Animal Care Committee of USTC First Affiliated Hospital approved all animal protocols (No. 2023-N(A)-001), and the study was carried out in compliance with ARRIVE guidelines.

Acknowledgment

We thankfully acknowledge and appreciate the Medical Research Center and the Institute of Geriatric Medicine at USTC first affiliated hospital team for their kind support during this study and provision of platform and technical support. Besides we are also thankful to Dr Dexin Shen at Urology department of this hospital for his technical support during this study.

Funding

This study was carried out with the support of National Natural Science foundation of China (under Grant numbers 82072807), University Scientific research Project of the Education department of Anhui Province (Grant numbers 2022AH051256) and Huai'an Natural Science Foundation (Grant numbers HAB202107).

Conflict of Interest

The authors declare no conflict of interest.

Supplementary Material

Supplementary material associated with this article can be found, in the online version, at https://doi.org/10.31083/FBL38061.

References

- [1] Xia C, Dong X, Li H, Cao M, Sun D, He S, et al. Cancer statistics in China and United States, 2022: profiles, trends, and determinants. Chinese Medical Journal. 2022; 135: 584–590. https://doi.org/10.1097/CM9.000000000002108.
- [2] Kang MJ, Won YJ, Lee JJ, Jung KW, Kim HJ, Kong HJ, et al.

- Cancer Statistics in Korea: Incidence, Mortality, Survival, and Prevalence in 2019. Cancer Research and Treatment. 2022; 54: 330–344. https://doi.org/10.4143/crt.2022.128.
- [3] Siegel RL, Miller KD, Fuchs HE, Jemal A. Cancer statistics, 2022. CA. 2022; 72: 7–33. https://doi.org/10.3322/caac.21708.
- [4] Capitanio U, Bensalah K, Bex A, Boorjian SA, Bray F, Coleman J, et al. Epidemiology of Renal Cell Carcinoma. European Urology. 2019; 75: 74–84. https://doi.org/10.1016/j.eururo.2018.08.036.
- [5] Kocarnik JM, Compton K, Dean FE, Fu W, Gaw BL, Henrikson HJ, et al. Cancer Incidence, Mortality, Years of Life Lost, Years Lived With Disability, and Disability-Adjusted Life Years for 29 Cancer Groups From 2010 to 2019: A Systematic Analysis for the Global Burden of Disease Study 2019. JAMA Oncology. 2022; 8: 420–444. https://doi.org/10.1001/jamaoncol. 2021.6987.
- [6] Moch H, Amin MB, Berney DM, Compérat EM, Gill AJ, Hartmann A, et al. The 2022 World Health Organization Classification of Tumours of the Urinary System and Male Genital Organs-Part A: Renal, Penile, and Testicular Tumours. European Urology. 2022; 82: 458–468. https://doi.org/10.1016/j.eururo.2022.06.016.
- [7] Huang P, Cao Q, Xu M, Dong XP. Lysosomal ATP Transporter SLC17A9 Controls Cell Viability via Regulating Cathepsin D. Cells. 2022; 11: 887. https://doi.org/10.3390/cells11050887.
- [8] Cao Q, Zhao K, Zhong XZ, Zou Y, Yu H, Huang P, et al. SLC17A9 protein functions as a lysosomal ATP transporter and regulates cell viability. The Journal of Biological Chemistry. 2014; 289: 23189–23199. https://doi.org/10.1074/jbc.M114. 567107
- [9] Wu J, Yang Y, Song J. Expression of SLC17A9 in hepatocellular carcinoma and its clinical significance. Oncology Letters. 2020; 20: 182. https://doi.org/10.3892/ol.2020.12043.
- [10] Yang L, Chen Z, Xiong W, Ren H, Zhai E, Xu K, *et al.* High expression of SLC17A9 correlates with poor prognosis in colorectal cancer. Human Pathology. 2019; 84: 62–70. https://doi.org/10.1016/j.humpath.2018.09.002.
- [11] Mi YY, Sun CY, Zhang LF, Wang J, Shao HB, Qin F, et al. Long Non-coding RNAs LINC01679 as a Competitive Endogenous RNAs Inhibits the Development and Progression of Prostate Cancer via Regulating the miR-3150a-3p/SLC17A9 Axis. Frontiers in Cell and Developmental Biology. 2021; 9: 737812. https://doi.org/10.3389/fcell.2021.737812.
- [12] Sun M, Qiu J, Zhai H, Wang Y, Ma P, Li M, et al. Prognostic Implications of Novel Gene Signatures in Gastric Cancer Microenvironment. Medical Science Monitor: International Medical Journal of Experimental and Clinical Research. 2020; 26: e924604. https://doi.org/10.12659/MSM.924604.
- [13] Hasuzawa N, Tatsushima K, Tokubuchi R, Kabashima M, Nomura M. VNUT Is a Therapeutic Target for Type 2 Diabetes and NASH. Yakugaku Zasshi. 2021; 141: 517–526. https://doi.org/10.1248/yakushi.20-00204-4. (In Japanese)
- [14] Hasuzawa N, Tatsushima K, Wang L, Kabashima M, Tokubuchi R, Nagayama A, et al. Clodronate, an inhibitor of the vesicular nucleotide transporter, ameliorates steatohepatitis and acute liver injury. Scientific Reports. 2021; 11: 5192. https://doi.org/10.1038/s41598-021-83144-w.
- [15] Kinoshita M, Hirayama Y, Fujishita K, Shibata K, Shinozaki Y, Shigetomi E, et al. Anti-Depressant Fluoxetine Reveals its Therapeutic Effect Via Astrocytes. EBioMedicine. 2018; 32: 72–83. https://doi.org/10.1016/j.ebiom.2018.05.036.
- [16] Hemmerlein B, Weseloh RM, Mello de Queiroz F, Knötgen H, Sánchez A, Rubio ME, et al. Overexpression of Eag1 potassium channels in clinical tumours. Molecular Cancer. 2006; 5: 41. https://doi.org/10.1186/1476-4598-5-41.
- [17] Camacho J. Ether à go-go potassium channels and cancer. Can-



- cer Letters. 2006; 233: 1–9. https://doi.org/10.1016/j.canlet.2005.02.016.
- [18] Pardo LA, Stühmer W. Eag1: an emerging oncological target. Cancer Research. 2008; 68: 1611–1613. https://doi.org/10.1158/0008-5472.CAN-07-5710.
- [19] Pardo LA, Sühmer W. Eag1 as a cancer target. Expert Opinion on Therapeutic Targets. 2008; 12: 837–843. https://doi.org/10. 1517/14728222.12.7.837.
- [20] Farias LMB, Ocaña DB, Díaz L, Larrea F, Avila-Chávez E, Cadena A, et al. Ether a go-go potassium channels as human cervical cancer markers. Cancer Research. 2004; 64: 6996–7001. https://doi.org/10.1158/0008-5472.CAN-04-1204.
- [21] Ortiz CS, Montante-Montes D, Saqui-Salces M, Hinojosa LM, Gamboa-Dominguez A, Hernández-Gallegos E, et al. Eagl potassium channels as markers of cervical dysplasia. Oncology Reports. 2011; 26: 1377–1383. https://doi.org/10.3892/or.2011. 1441.
- [22] Zhang Z, Lin E, Zhuang H, Xie L, Feng X, Liu J, et al. Construction of a novel gene-based model for prognosis prediction of clear cell renal cell carcinoma. Cancer Cell International. 2020; 20: 27. https://doi.org/10.1186/s12935-020-1113-6.
- [23] Masuda T, Ozono Y, Mikuriya S, Kohro Y, Tozaki-Saitoh H, Iwatsuki K, et al. Dorsal horn neurons release extracellular ATP in a VNUT-dependent manner that underlies neuropathic pain. Nature Communications. 2016; 7: 12529. https://doi.org/10. 1038/ncomms12529.
- [24] Soeda M, Ohka S, Nishizawa D, Hasegawa J, Nakayama K, Ebata Y, et al. Single-nucleotide polymorphisms of the SLC17A9 and P2RY12 genes are significantly associated with phantom tooth pain. Molecular Pain. 2022; 18: 17448069221089592. https://doi.org/10.1177/17448069221089592.
- [25] Sillars-Hardebol AH, Carvalho B, Tijssen M, Beliën JAM, de Wit M, Delis-van Diemen PM, et al. TPX2 and AURKA promote 20q amplicon-driven colorectal adenoma to carcinoma progression. Gut. 2012; 61: 1568–1575. https://doi.org/10.1136/ gutjnl-2011-301153.
- [26] Chen B, Jiang L, Zhong ML, Li JF, Li BS, Peng LJ, et al. Identification of fusion genes and characterization of transcriptome features in T-cell acute lymphoblastic leukemia. Proceedings of the National Academy of Sciences of the United States of America. 2018; 115: 373–378. https://doi.org/10.1073/pnas.1717125115.
- [27] Gao Y, Chen Y, Liu M, Zeng D, Tan F, Wan H, *et al.* SLC17A9 as a prognostic biomarker correlated with immune infiltrates in human non-small cell lung cancer. American Journal of Cancer Research. 2023; 13: 3963–3982.
- [28] Takai E, Tsukimoto M, Harada H, Sawada K, Moriyama Y, Kojima S. Autocrine regulation of TGF-β1-induced cell migration by exocytosis of ATP and activation of P2 receptors in human

- lung cancer cells. Journal of Cell Science. 2012; 125: 5051–5060. https://doi.org/10.1242/jcs.104976.
- [29] Kui XY, Gao Y, Liu XS, Zeng J, Yang JW, Zhou LM, et al. Comprehensive Analysis of SLC17A9 and Its Prognostic Value in Hepatocellular Carcinoma. Frontiers in Oncology. 2022; 12: 809847. https://doi.org/10.3389/fonc.2022.809847.
- [30] Li W, Xu N, Meng X, Yuan H, Yu T, Miao Q, et al. SLC17A9-PTHLH-EMT axis promotes proliferation and invasion of clear renal cell carcinoma. iScience. 2023; 26: 105764. https://doi.or g/10.1016/j.isci.2022.105764.
- [31] Li JK, Chen C, Liu JY, Shi JZ, Liu SP, Liu B, *et al.* Long non-coding RNA MRCCAT1 promotes metastasis of clear cell renal cell carcinoma via inhibiting NPR3 and activating p38-MAPK signaling. Molecular Cancer. 2017; 16: 111. https://doi.org/10.1186/s12943-017-0681-0.
- [32] Cao M, Nawalaniec K, Ajay AK, Luo Y, Moench R, Jin Y, et al. PDE4D targeting enhances anti-tumor effects of sorafenib in clear cell renal cell carcinoma and attenuates MAPK/ERK signaling in a CRAF-dependent manner. Translational Oncology. 2022; 19: 101377. https://doi.org/10.1016/j.tranon.2022.101377.
- [33] Mello de Queiroz F, Suarez-Kurtz G, Stühmer W, Pardo LA. Ether à go-go potassium channel expression in soft tissue sarcoma patients. Molecular Cancer. 2006; 5: 42. https://doi.org/ 10.1186/1476-4598-5-42.
- [34] Petroni G, Bagni G, Iorio J, Duranti C, Lottini T, Stefanini M, et al. Clarithromycin inhibits autophagy in colorectal cancer by regulating the hERG1 potassium channel interaction with PI3K. Cell Death & Disease. 2020; 11: 161. https://doi.org/10.1038/s41419-020-2349-8.
- [35] Bai Y, Liao H, Liu T, Zeng X, Xiao F, Luo L, *et al.* MiR-296-3p regulates cell growth and multi-drug resistance of human glioblastoma by targeting ether-à-go-go (EAG1). European Journal of Cancer (Oxford, England: 1990). 2013; 49: 710–724. https://doi.org/10.1016/j.ejca.2012.08.020.
- [36] Chen J, Xuan Z, Song W, Han W, Chen H, Du Y, et al. EAG1 enhances hepatocellular carcinoma proliferation by modulating SKP2 and metastasis through pseudopod formation. Oncogene. 2021; 40: 163–176. https://doi.org/10.1038/s41388-020-01522-6.
- [37] Menéndez ST, Rodrigo JP, Alvarez-Teijeiro S, Villaronga MÁ, Allonca E, Vallina A, *et al.* Role of HERG1 potassium channel in both malignant transformation and disease progression in head and neck carcinomas. Modern Pathology. 2012; 25: 1069–1078. https://doi.org/10.1038/modpathol.2012.63.
- [38] Goodman AD, Brown TR, Krupp LB, Schapiro RT, Schwid SR, Cohen R, *et al.* Sustained-release oral fampridine in multiple sclerosis: a randomised, double-blind, controlled trial. Lancet (London, England). 2009; 373: 732–738. https://doi.org/10.1016/S0140-6736(09)60442-6.

